

**Fundamental- and first-order localized states in a cubic-quintic reaction-diffusion system**

P. V. Paulau

*TU Berlin, Institute for Theoretical Physics, Hardenbergstrasse 36, Sekr EW 7-1, 10623 Berlin, Germany*  
*and Carl-von-Ossietzky University of Oldenburg, Institute for Chemistry and Biology of the Marine Environment (ICBM),*  
*Carl-von-Ossietzky-Strasse 9-11, 26111 Oldenburg, Germany*

(Received 23 September 2013; published 13 March 2014)

This article analyzes the properties of rotationally symmetric self-localized solutions with different radial quantum numbers in the simplest one- and two-component reaction-diffusion systems. The consideration is made in one and two dimensions with the focus on the fundamental and first higher-order solutions showing zero and one intersections of the radial profile with zero. It is demonstrated that the solution with one intersection does not exist for the case of the quadratic-cubic nonlinearity, while the cubic-quintic extension of the models does allow existence. I show additionally that the cubic-quintic reaction diffusion system supports the existence and stability of the states with zero quantum numbers, as well as their antistates, state-antistate pairs, and clusters, which can be interpreted as the states with nonzero azimuthal quantum number.

DOI: [10.1103/PhysRevE.89.032910](https://doi.org/10.1103/PhysRevE.89.032910)

PACS number(s): 82.40.Ck

**I. INTRODUCTION**

Reaction diffusion (RD) systems display a rich variety of spatiotemporal patterns [1,2]. Though the real reactions are of significant complexity, it was a great achievement to formulate the simplest phenomenological models [3,4], explaining the key phenomena, such as front propagation [5], Turing pattern [6], and solitary waves [7]. A number of phenomena, however, cannot be captured after a sequence of simplifications. For example, the one-component system (Schloegl also Zeldovich-Frank-Kamenetskii) displays only the stable front propagation, while the two-component extension gives rise to the stable pulse propagation, and a third component allows even more complicated phenomena such as two-dimensional stable traveling pulse [8], pacemaker [9], bistability of moving pulses [9], breathing solitons [10], radial spots [11]. Another way toward complexity in the simplest one-component equation is to add additional spatial couplings, e.g., nonlocality, which makes it analogous to the Swift-Hohenberg equation accordingly with existence of resting localized states, including the radial spots and rings [12].

While the existence and stability of the dissipative self-localized states with nonzero azimuthal numbers is well established (see, e.g., Refs. [13–15]), the corresponding questions for higher radial numbers (i.e., number of intersections of the radial profile with zero) still remain unclear and serve as motivation of this work. One needs to note that, in contrast to the well-established dissipative solitons with snaking bifurcation diagram [12,16], the solutions considered below have a finite (and small) number of zeros in radial profile.

One of the starting points here is taken from Refs. [17,18], where qualitatively new solutions appear due to the increase of dimensionality (i.e., merely due to the  $\frac{1}{r} \frac{\partial}{\partial r}$  term), rather than due to different mechanism of localization connected with Turing patterns and locking of fronts between modulated and homogeneous solutions possible even in one dimension (see, e.g., Refs. [12,19] for Swift-Hohenberg equation, Refs. [20,21] for optical solitons, and Ref. [22] for localized structures in dryland vegetation). The challenge is that the stable forms of the dimension-induced states with nonzero radial quantum number are not found in the literature (see, e.g., Refs. [23,24]).

This article hopes to stimulate efforts to find azimuthal, radial, and possibly orbital (if 3D) quantization in the context of solitons in diverse dissipative systems as well as to find conditions that would provide the stability.

The existence of states with radial number 0 and 1, as well as of the “antistates” (solutions with opposite sign with respect to the states) and “state-antistate” pairs is demonstrated for cubic-quintic RD systems. In contrast to the states in the conservative systems (e.g., nonlinear Schroedinger equation) the states studied here are discrete. In contrast to conventional dissipative systems such as cubic-quintic Ginzburg-Landau equation [25], there is no invariance with respect to phase rotation (gauge), i.e., the antistate is “more” discrete and cannot be transformed into its state via continuous phase transformation, what makes the system very attractive for following studies.

Similar to Refs. [8–11] developing the three-component RD model, my aim is to add to the understanding of the quintic reaction diffusion system previously explored only in the context of the front propagation [26]. I hope that the interdisciplinary starting points will make it possible to develop the more powerful studies concerning the quantization of dissipative solitons, including consideration of practically important systems. This hope is supported by the diversity of possible control techniques [27–29], including nonlocality [30–33], delayed feedback [34–36], or external forcing [37].

In Sec. II, the relation between the simplest one-dimensional localized solutions of the nonlinear Schroedinger equation (NSE) and of the RD models is demonstrated. In Sec. III, I consider the two-dimensional fundamental and higher-order states of the nonlinear Schroedinger equation and their continuation toward the reaction-diffusion case. The impossibility of the higher-order states is demonstrated and explained, and the need to deal with higher nonlinearities is discussed. In Sec. IV, the reaction-diffusion model is extended by cubic-quintic nonlinearity. The existence of the fundamental localized state, antistate, higher-order symmetric, and asymmetric state is demonstrated. Section V gives conclusions.

## II. FITZHUGH NAGUMO AND NONLINEAR SCHRÖDINGER EQUATIONS

The FitzHugh-Nagumo model (FHN) is the simplest two-component model of fundamental importance in the theory of reaction diffusion systems. Beside the phenomena, already explained by the single-component models (see, e.g., Ref. [5]), it also explains the phenomena of excitability and oscillatory behavior inherent to the processes in nerve cells. It demonstrates the phenomena of excitation pulse propagation and the spiral solutions—generic patterns in excitable media, which are also observed in chemical reactions and their models. Here the following form of FHN model is used:

$$\begin{aligned}\dot{u} &= f_{11}u + f_{12}v + f_2u^2 + f_3u^3 + \Delta u, \\ \dot{v} &= f_{21}u + f_{22}v,\end{aligned}\quad (1)$$

where  $u$  and  $v$  are real (space dependent) quantities (concentrations),  $\Delta$  is Laplace operator, the space is normalized to have diffusion constant equal 1, and all coefficients are real numbers. The consideration is made in one and two dimensions and each choice is specified below. These notations are used because they make it possible to change the nonlinearity parameters independently and it is easy to find connection with other notations in the literature. Let us write down the steady-state ( $\dot{u} = 0, \dot{v} = 0$ ) condition for system Eq. (1):

$$0 = f_1u + f_2u^2 + f_3u^3 + \Delta u, \quad (2)$$

where  $f_1 = \frac{f_{11}f_{22} - f_{21}f_{12}}{f_{22}}$ .

The aim is to find relation between the solutions of the reaction-diffusion systems and the nonlinear Schrödinger equation. The latter appears in various branches of physics [38]:

$$\dot{\Psi} = i\Delta\Psi + i|\Psi|^2\Psi, \quad (3)$$

where  $\Psi$  is the complex variable and the sign of nonlinearity is chosen to allow the existence of soliton solutions. Searching the stationary solutions of Eq. (3) of the form  $\Psi = u(\mathbf{r})e^{-if_1t}$ , one obtains the following equation for real (space dependent) quantity  $u$ :

$$0 = f_1u + u^3 + \Delta u, \quad (4)$$

where the same symbols  $u$  and  $f_1$  are used as in FHN model, although they have completely different meanings. Formally, Eq. (4) is equivalent to Eq. (2) with specific choice of parameters:  $f_2 = 0, f_3 = 1$ . This choice of parameters of RD system means that it will explode to infinity at sufficiently large perturbation, since the highest nonlinearity does not provide saturation. I will continue, however, the consideration with the aim to connect these two cases.

Though there are no general ways to find analytical solutions of nonlinear equations, Eq. (2) is one of those rare cases for which the analytical localized solution is known when one-dimensional space is considered  $\Delta = \frac{\partial^2}{\partial x^2}$  [39]. It has the form

$$u = \frac{A}{B + C \cosh(kx)}, \quad (5)$$

where  $A, B, C$ , and  $k$  are  $x$ -independent constants. Simply substituting Eq. (5) into Eq. (2), one can obtain several

algebraic conditions, from which one can express

$$k = \pm\sqrt{-f_1}, \quad A = \frac{3f_1B}{f_2}, \quad C = \pm\frac{B}{f_2}\sqrt{f_2^2 - \frac{9f_3f_1}{2}}, \quad (6)$$

where the bottom index is always the parameter index, while the top index is the power. Note, that  $A, B$ , and  $C$  are not independent and actually  $B$  is canceled after substitution of Eq. (6) into Eq. (5). So we have

$$u = \frac{-3f_1}{f_2 + \sqrt{f_2^2 - \frac{9f_3f_1}{2}} \cosh(\sqrt{-f_1}x)}. \quad (7)$$

The choice of sign for  $k$  in Eq. (6) is arbitrary, it reflects only the parity symmetry. For a localized solution, the plus sign should be chosen for  $C$ ; otherwise, the discontinuous solution will be considered. For  $f_2 = 0$ , Eq. (7) transforms exactly to the classical  $\text{sech}(kx)$  solution of NSE, which exists only for  $f_3 > 0$  and  $f_1 < 0$  as follows from Eq. (7).

To be consistent, one needs to define the choice of parameters. We take them to have exact correspondence to the excitability case, considered in Ref. [40], so that

$$\begin{aligned}f_{11} &= -0.045, & f_{12} &= -1.0, & f_{21} &= 0.015, \\ f_{22} &= -0.0525, & f_2 &= 1.045, & f_3 &= -1.\end{aligned}\quad (8)$$

Excitability means that there should be only one homogeneous solution ( $u = 0, v = 0$  in our case), it should be stable (positive determinant and negative trace of linear matrix  $f_{ij}$ ), and the dynamics should demonstrate the long-term excursion, when the perturbation is large enough.

The parameters responsible for the linear part are kept fixed everywhere throughout the article. The task of interest now is to follow the transition from the nonlinear Schrödinger case ( $f_2 = 0, f_3 = 1$ ) to the typical FitzHugh-Nagumo case ( $f_2 = 1.045, f_3 = -1$ ). The change of the maximum of soliton Eq. (7) is shown in Fig. 1 for continuous transformation of nonlinearity parameters. First, the  $f_2$  coefficient was changed gradually, starting from  $O$  ( $f_2 = 0, f_3 = 1$ ) and moving to  $P$  ( $f_2 = 1.045$  and  $f_3 = 1$ ). Second, we move from  $P$  to  $Q$ , changing  $f_3$  and keeping other parameters fixed. The plotted  $OPQ$  branch has meaning for conservative case of NSE with quadratic and cubic nonlinearity both for positive and for negative values of  $f_3$ , while the only part of the branch for negative  $f_3$  is meaningful for dissipative reaction-diffusion system for saturation reasons. The zero (dashed thin line) and nonzero (solid thin line) homogeneous steady state solutions of Eq. (2) are plotted in Fig. 1. It can be seen that the localized separatrix  $OPQ$  does exist not for the whole region of existence of nonzero homogeneous state and clearly not in the region of excitability, corresponding to  $f_3 = -1$ . Moreover, approaching the point  $Q$  the separatrix solution transforms to the very broad plateau, which looks like two fronts, which makes it difficult to distinguish between critical front [41] and critical nucleus, since it is still the localized object, though with very steep shape.

The above consideration has been presented because it is analytical, but it helps little since the discussed state is typically unstable. The stability can be reached, however, when we consider more complex systems, which can additionally support the Turing patterns and stable motionless one- and

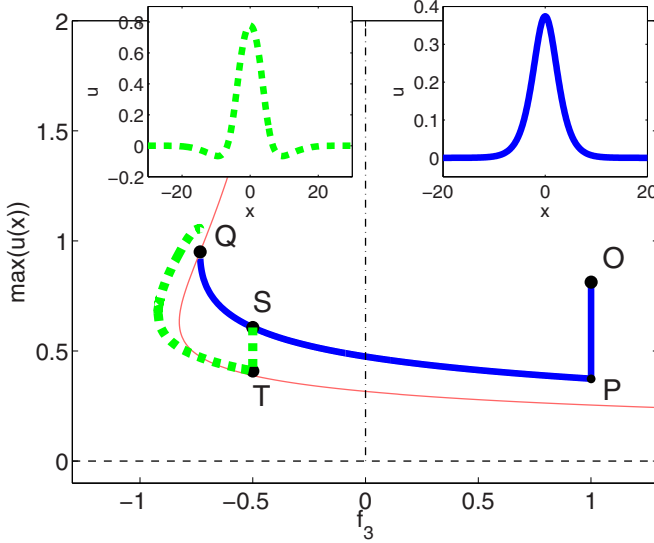


FIG. 1. (Color online) Bifurcation diagram. Solid thin (red) line is the branch of homogeneous solutions ( $0 = f_1u + f_2u^2 + f_3u^3$ ). Solid bold line OPQ represents the branch of spatially localized 1D solutions Eq. (7). Dashed thin line (coincides with abscissa) is the trivial homogeneous solution. Vertical dash-dotted line marks  $f_3 = 0$ . The dashed bold (green) line represents the localized solution in the presence of inhibitor diffusion. Choice and change of parameters are explained in text. Right inset shows the form of Eq. (7), qualitatively identical for all OPQ branch. The left inset shows the typical form of localized state in the presence of inhibitor diffusion.

multidimensional localized states:

$$\begin{aligned} \dot{u} &= f_{11}u + f_{12}v + f_2u^2 + f_3u^3 + \Delta u, \\ \dot{v} &= (f_{21}u + f_{22}v + D_v \Delta v) \frac{1}{\varepsilon}, \end{aligned} \quad (9)$$

where in contrast to Eqs. (1) the inhibitor diffusion  $D_v \Delta v$  is added. It is convenient to add the additional parameter  $\varepsilon$  since it has influence only on the stability of resting states but not on their shape and existence. We can show now how  $D_v$  makes it possible to make a fold in the shape of the critical nucleus branch. To do so, we start from solution marked by point S ( $f_2 = 1.045, f_3 = -0.5, D_v = 0.0$ ) in Fig. 1 and follow it using a Newton-Raphson continuation to the point T with ( $f_2 = 1.045, f_3 = -0.5, D_v = 1.0$ ). The branch with the saddle node bifurcation is formed by change of  $f_3$  (dashed bold line to the left from the point T). Both top and bottom branches of the folded curve are unstable for a slow inhibitor, e.g., for  $\varepsilon = 1.0$ . It seems that this unstable solution is the “hidden” solution (also called “scatter”), which was found and discussed in Ref. [40]. It can become stable (and hence “not hidden”) just by choosing a sufficiently fast inhibitor relaxation rate, e.g.,  $\varepsilon = 0.1$  and it is broadly studied, since it represents the localized patch of the Turing pattern.

### III. HIGHER-ORDER STATES AND THEIR CONTINUATION

The nonlinear Schroedinger equation is one of the fundamental equations of physics and has been studied very

well. For the aims of this article, one needs to add that the one-dimensional bright-soliton solution (discussed above) is unique and no more bright solitons exist in 1D. When NSE is two-dimensional, the two new families characterized by discrete numbers appear. These are the localized vortex solutions with discrete rotational symmetry and phase singularity and the localized solutions with circular symmetry. One should note, however, that these solutions are unstable. The Townes soliton [42] can be stabilized by the nonlocal coupling [30]. This is in agreement with the modern trends of control techniques in RD systems [27]. Let us consider first the circularly symmetric solutions. This means, we can choose the polar coordinate system  $(r, \phi)$ , connected with the symmetry center of solution and the derivative  $\frac{\partial}{\partial \phi} = 0$ . Now,

$$\Delta = \frac{\partial^2 u}{\partial r^2} + \frac{1}{r} \frac{\partial u}{\partial r}$$

can be used in Eq. (2). There are no analytical solutions for the 2D case and the numerical shooting method is used to find the profiles. One introduces the new variable  $U = \frac{\partial u}{\partial r}$ , then Eq. (2) with radial Laplacian is transformed to the system

$$\frac{\partial U}{\partial r} = -f_1u - f_2u^2 - f_3u^3 - \frac{1}{r}U, \quad \frac{\partial u}{\partial r} = U. \quad (10)$$

Interpreting  $r$  as dynamic variable one can solve system Eq. (10) numerically, e.g., using Euler or Runge-Kutta method for different initial conditions  $u(0)$  and  $U(0)$ . The solutions of our interest with radial symmetry have a maximum in  $r = 0$ ; hence, we always take  $U(0) = 0$  and run through all possible (reasonable) values of  $u(0)$ . This dynamic system is tricky, since zero solution ( $u = 0, U = 0$ ) is always unstable because of parity symmetry, which may look broken due to  $\frac{1}{r} \frac{\partial u}{\partial r}$  term, but in the limit  $r \rightarrow \infty$  there is parity. Nevertheless, one can find solutions with  $u(r) \rightarrow 0$  at  $r \rightarrow +\infty$  with rather good precision, omitting the exponentially growing part which appears for high  $r$ . For the nonlinear Schroedinger equation, the sequence of circularly symmetric solutions has been found in the 1960s [17,18] and we basically reproduce those results solving Eq. (10) with  $f_2 = 0$  and  $f_3 = 1$ . Our interest, however, goes further into the qualitatively different case of reaction diffusion systems; therefore, we follow again the way of previous section. Again, one cannot do this analytically and the Newton continuation is used. The first and second derivatives over  $r$  are calculated using the second-order finite difference formula. The l’Hôpital’s rule is used to calculate  $\frac{1}{r} \frac{\partial u}{\partial r}$  in special point  $r = 0$ . Starting from the solutions of the nonlinear Schroedinger equation, marked by points  $O_0, O_1$ , changing quadratic nonlinearity coefficient  $f_2$  from 0 to 1.045 the transformation of the states is followed toward points  $P_0, P_1$  in Fig. 2 (see also insets of Fig. 2). The index near the point means here the number of intersections of the radial profile with zero, i.e., the “radial quantum number of soliton.” In the next step the parameter  $f_3$  was changed from 1.0 toward negative values, relevant for RD systems. As one can see from Fig. 2, the behavior of the fundamental (no intersections of radial profile with zero) soliton ( $O_0, P_0, Q_0$ ) is qualitatively the same as the behavior of the 1D soliton considered in the previous section. The higher-order solution behaves differently. First, there is an increase of amplitude during addition of positive quadratic nonlinearity. Second, the

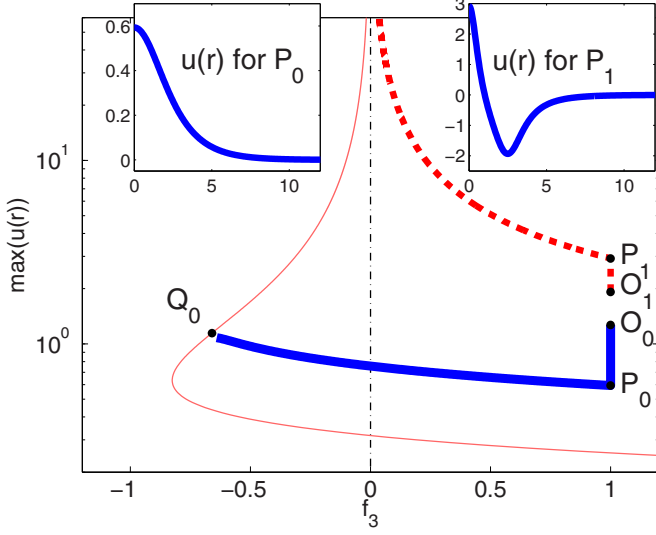


FIG. 2. (Color online) Bifurcation diagram for spatially localized, rotationally symmetric 2D solutions of Eq. (2). The solid thin gray (red) line is the nonzero homogeneous solution (the same as described in the legend of Fig. 1, but in semilog scale). The solid bold (blue) line is the dependence of  $\max(u)$  on  $f_3$  for the fundamental soliton, whose radial profile is given in the left inset (index 0 near the symbol of points). The dashed (red) line is the dependence of  $\max(u)$  on  $f_3$  for the first higher-order soliton, whose radial profile is given in the right inset (index 1 near the symbols of points). Points  $O_j, P_j, Q_j$  are analogous to points  $O, P, Q$  of Fig. 1 and described in text. Vertical dash-dotted line (ordinate axis) marks  $f_3 = 0$ , the asymptote for higher-order states and the border between reaction-diffusion and the Schroedinger case.

amplitude tends asymptotically to infinity at  $f_3 \rightarrow +0$ . This can be explained by the presence of regions with negative  $u$  as illustrated in the right inset of Fig. 2 and by the fact that the quadratic nonlinearity does not provide saturation for negatively defined  $u$ . One needs to emphasize, however, that the seemingly similar case of states presented in the left inset of Fig. 1 is qualitatively different from the case of the higher-order radial states. First, because of mechanisms responsible for the formation of these states (dimensionality versus inhibitor diffusion). Second, because of the qualitative and quantitative properties of these states (e.g., the number of intersections with zero and the relative depth of the first minimum). Third, because of the existence ranges of the states (the one can be observed in RD system with positive quadratic and negative cubic nonlinearity, the other cannot).

For positively defined solutions (both 1D and 2D), it was not crucial which nonlinearity leads to saturation, and solutions exist also for purely quadratic nonlinearity as follows from intersection of  $PQ$  curve with dash-dotted line in Fig. 1 or from corresponding intersection in Fig. 2. To finish this section, we note that analogously to the one-dimensional case, the stabilization of the fundamental two-dimensional (initially bell-like) soliton is possible using the model with diffusing inhibitor Eq. (9). The higher-order solution for positively defined  $D_v$  and  $f_2$  can still not overcome  $f_3 = 0$  asymptote, and we come to the phenomenological model with odd powers discussed in the next section.

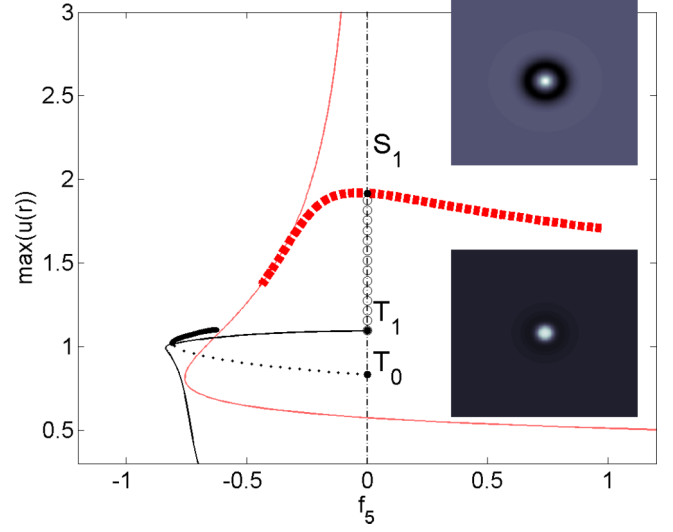


FIG. 3. (Color online) Bifurcation diagram of the solutions to the cubic-quintic RD model Eq. (11). Linear parameters are fixed everywhere to values defined in Eq. (8). The dashed bold (red) line represents the branch of the first higher-order radial solution for  $f_3 = 1, D_v = 0.0$ . The solid thin gray (red) line represents the homogeneous nontrivial steady state. The branch  $S_1 T_1$  (again index 1 means “first” higher-order state) marked by circles corresponds to the change of  $D_v$  from 0 to 2.0. The branch starting from  $T_1$  and marked by solid thin line corresponds to the change of  $f_5$  with fixed  $f_3 = 1$  and  $D_v = 2$ . The dotted line starting from  $T_0$  ( $f_3 = 1, D_v = 2$ ) corresponds to the unstable fundamental soliton, which became stable above the fold point (for small enough  $\varepsilon$ ). The corresponding stable branch is marked by a bold black line. The top and bottom inset shows the 2D profile of  $u$  near the fold for higher-order and fundamental states, respectively.

#### IV. REACTION-DIFFUSION SYSTEMS WITH QUINTIC NONLINEARITY

Let us use the phenomenological model [26] including cubic and quintic terms:

$$\begin{aligned} \dot{u} &= f_{11}u + f_{12}v + f_3u^3 + f_5u^5 + \Delta u, \\ \dot{v} &= (f_{21}u + f_{22}v + D_v\Delta v)\frac{1}{\varepsilon}. \end{aligned} \quad (11)$$

In contrast to the model Eqs. (1) and (9), the role of quadratic nonlinearity is now played by the cubic term, while the role of saturating nonlinearity is played by the quintic term. The classical nonlinear Schroedinger case corresponds to  $f_3 = 1.0, f_5 = 0.0$ , and  $D_v = 0.0$ . Starting again from these parameters, the higher-order radial solution was traced changing the only  $f_5$  coefficient. The corresponding branch is shown by a bold dashed (red) line in Fig. 3. The profile of the higher-order state before and after this transformation (toward negative  $f_5$ ) is shown in Fig. 4(b). One can see that, similar to the separatrix solutions  $OPQ$  in Fig. 1 and  $O_0P_0Q_0$  of Fig. 2, the branch hits the curve of homogeneous solution. The same also happens with fundamental Townes soliton or critical nucleus, whose branch is not shown for simplicity in Fig. 3, but the profiles for the initial case of  $f_5 = 0.0$  and for the case close to hitting the homogeneous state are shown in Fig. 4(a). It means that incorporation of fifth-order nonlinearity does not

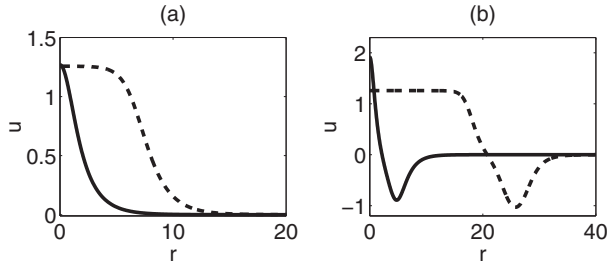


FIG. 4. The transformation of solutions of Eq. (11) at variation of quintic nonlinearity. Solid lines  $f_5 = 0$ , dashed lines  $f_5 = -0.5$ , the linear parameters are fixed in Eq. (8),  $f_3 = 1$ ,  $D_v = 0$ . (a) Fundamental self-localized state, (b) first higher-order self-localized state.

kill the phenomena, which exists even for zero  $D_v$ . Even small negative values of  $f_5$  make the solution meaningful for the reaction diffusion case, since there is no unsaturated growth any more. Figure 4 demonstrates how the two 2D solutions with radial numbers 0 and 1 are deformed changing  $f_5$  from 0 to  $-0.5$ . One can see that the quintic nonlinearity introduces a kind of threshold, forming a plateau in the profile of states. These states remain unstable for the cubic-quintic setting, but in contrast to typical azimuthal instability [23], the mode with maximum growth rate has the continuous rotational symmetry.

It is reasonable to consider here the influence of the inhibitor diffusion. Similar to the case of the one-dimensional soliton, starting from the radial higher-order state (point  $S_1$  in Fig. 3) for  $D_v = 0$ ,  $f_5 = 0$ , the point  $T_1$  was reached by increase of  $D_v$  till 2.0, keeping other parameters fixed (see empty circles in Fig. 3). Next, starting from the state  $T_1$ , changing  $f_5$  coefficient and keeping all other parameters fixed (see thin solid black line in Fig. 3), the whole branch with the fold point was obtained! Despite the fold point, the branch remains unstable, however, and needs further studies.

The analogous procedure is performed for fundamental soliton. Point  $T_0$  (in Fig. 3) corresponds to  $D_v = 2$  and the dotted line represents the unstable branch of “critical nucleus,” while the state is stable above the fold point (the bold solid black line). The last is valid for small enough  $\varepsilon$ . The instability due to the dynamics of  $v$  is out of interest here because the aim is actually to get stable states and one can consider the limit of small  $\varepsilon$ , when the equation for  $v$  can be adiabatically eliminated with the resulting one-component nonlocal system:

$$\dot{u} = f_1 u + f_3 u^3 + f_5 u^5 + \Delta u + \hat{G}u, \quad (12)$$

where operator  $\hat{G}$  can be directly represented in Fourier space via

$$\hat{G}u(\mathbf{r}) = F^{-1}\{F\{u(\mathbf{r})\}G(\mathbf{k})\}, \quad (13)$$

where  $F$  is direct Fourier transform, and  $F^{-1}$  is the inverse Fourier transform,

$$G(\mathbf{k}) = \frac{-f_{12}f_{21}D_v|\mathbf{k}|^2}{f_{22}(f_{22} - D_v|\mathbf{k}|^2)} \quad (14)$$

$$f_1 = \frac{f_{11}f_{22} - f_{12}f_{21}}{f_{22}}. \quad (15)$$

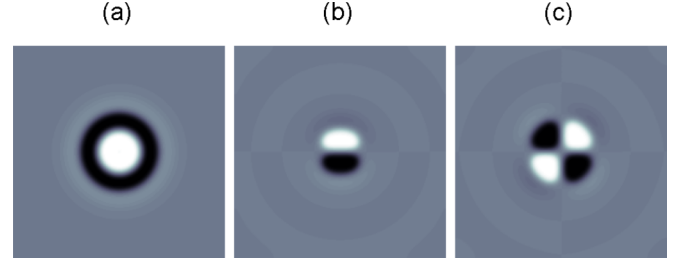


FIG. 5. (Color online) The stable localized solutions of Eq. (12) beyond the fundamental one. Parameters:  $f_3 = 1$ ,  $f_5 = -0.805$ ,  $D_v = 2$ ,  $f_1$  and  $G$  are defined via Eqs. (8), (14), and (15). (a) The symmetric radial localized state, (b) the bound state of soliton-antisoliton, (c) the bound state of two solitons-antisolitons. The more complex structures are typically unstable.

Or using the convolution theorem in real space:

$$\hat{G}u(\mathbf{r}) = \int_{-\infty}^{+\infty} G(|\mathbf{r} - \mathbf{s}|)u(\mathbf{s})d\mathbf{s}, \quad (16)$$

with  $G(|\mathbf{r}|) = F^{-1}\{G(\mathbf{k})\}$ .

The numerical time integration of the model Eq. (12) [and also of Eq. (11) with small  $\varepsilon$ ] reveals a number of stable localized patterns. First, the fundamental state (of the form shown in bottom inset of Fig. 3) and its antistate  $u(\mathbf{r}) = -u(\mathbf{r})$  are stable for the range of parameters discussed above (solid black bold line in Fig. 3). Second, the higher-order state (top inset of Fig. 3) is typically unstable and represents separatrix between attraction basins of different solutions. With small positive symmetric perturbation, the transition to the stable symmetric state shown in Fig. 5(a) is observed. However, this state does not belong to the folded branch marked by solid thin line in Fig. 3, and hence it is most likely the result of the Turing mechanism, rather than the mechanism of interest in this article. With small negative symmetric perturbation, the transition to the homogeneous zero solution is observed. If, however, strong enough random perturbation is applied, then the state evolves into the antisymmetric stable cluster shown in Fig. 5(b). The last resembles very much the profile of the vortex soliton of the nonlinear Schroedinger equation. Using the typical procedure of the vortex excitation [24] for the reaction diffusion system Eq. (12), more complex stable clusters, as shown in Fig. 5(c), are found. The clusters with the higher number of azimuthal periods are unstable.

## V. CONCLUSIONS

It is demonstrated that the profiles of the solutions of the nonlinear Schroedinger equation can be transformed to the profiles of solutions of the simplest reaction diffusion systems. In contrast to the fundamental soliton (i.e., without intersections of radial profile with zero), the more complex higher-order states with one zero of the radial profile cannot be transformed into solutions of the quadratic-cubic reaction diffusion system. The same is expected for higher radial numbers. One needs to note that the FitzHugh-Nagumo model Eq. (9) is the archetypical model for the study of the stationary self-localized states as patches of the Turing patterns, which can demonstrate also snaking and the analogy of

“higher-order” states discussed in this article. However, the existence (and stability) of patches of Turing patterns is created via the diffusion of inhibitor (or equivalently by nonlocal coupling), while the existence of the “higher-order” states in the NSE is provided exclusively by the transition  $\frac{\partial^2}{\partial x^2} \rightarrow \frac{\partial^2}{\partial r^2} + \frac{1}{r} \frac{\partial}{\partial r}$ , i.e., its nature is dimensionality, rather than other possible spatial couplings.

In contrast, the diverse localized states: fundamental state, higher-order state, bound state of soliton-antisoliton, and more complex clusters are found in the cubic-quintic reaction diffusion model (considered also in Ref. [26]).

Typically, there are many unstable states in pattern forming systems and we know much less about these than about the stable states. One would like to mention Refs. [40,43], where the nonlinearity is of a more complex form than considered here and the authors obtained the unstable states in a different

way. They were studying the collisions of moving pulses and noticed that in some situations there is a *long-living* resting state, formed during the collision process. Such a state is the *scatter* of one colliding pulse on another and it can be stabilized by choosing a sufficiently fast inhibitor relaxation rate. In contrast, the stabilization of the states obtained in this article is an intriguing and challenging task [34].

#### ACKNOWLEDGMENTS

This work was supported by the SFB 910. I am grateful to Natalia Loiko, Boris Malomed, Bernold Fiedler, Svetlana Gurevich, Thorsten Ackemann, Willie Firth, Damia Gomila, Jakob Loeber, and Harald Engel for useful discussions related to the subject of the article and Richard Holmes (Berlin) for assistance with the manuscript.

- 
- [1] M. C. Cross and P. C. Hohenberg, *Rev. Mod. Phys.* **65**, 851 (1993).
- [2] M. Cross and H. Greenside, *Pattern Formation and Dynamics in Nonequilibrium Systems* (Cambridge University Press, Cambridge, 2009).
- [3] F. Schloegl, *Z. Physik* **253**, 147 (1972).
- [4] R. FitzHugh, *Biophys. J.* **1**, 445 (1961); J. S. Nagumo, S. Arimoto, and S. Yoshizawa, *Proc. IRE* **50**, 2061 (1962).
- [5] A. S. Mikhailov, *Foundations of Synergetics I* (Springer, Berlin 1994).
- [6] A. M. Turing, *Phil. Trans. Roy. Soc. London B* **237**, 37 (1952).
- [7] H.-G. Purwins, H. U. Bödeker, and Sh. Amiranashvili, *Adv. Phys.* **59**, 485 (2010).
- [8] C. P. Schenk, M. Or-Guil, M. Bode, and H.-G. Purwins, *Phys. Rev. Lett.* **78**, 3781 (1997).
- [9] M. Stich, A. S. Mikhailov, and Y. Kuramoto, *Phys. Rev. E* **79**, 026110 (2009).
- [10] S. V. Gurevich, Sh. Amiranashvili, and H.-G. Purwins, *Phys. Rev. E* **74**, 066201 (2006).
- [11] P. van Heijster and S. Bjoern, *J. Nonlin. Sci.* **21**, 705 (2011).
- [12] D. Lloyd and B. Sandstede, *Nonlinearity* **22**, 485 (2009).
- [13] N. N. Rosanov, S. V. Fedorov, and A. N. Shatsev, *Phys. Rev. Lett.* **95**, 053903 (2005).
- [14] P. V. Paulau *et al.*, *Opt. Express* **18**, 8859 (2010).
- [15] J. Jimenez *et al.*, *J. Opt.* **15**, 044011 (2013).
- [16] W. J. Firth, L. Colombo, and T. Maggipinto, *Chaos* **17**, 037115 (2007).
- [17] Z. K. Yankauskas, *Izv. Vyssh. Uchebn. Zav. Radiofiz.* **9**, 412 (1966) [*Sov. Radiophys.* **9**, 261 (1966)].
- [18] H. A. Haus, *Appl. Phys. Lett.* **8**, 128 (1966).
- [19] D. Avitabile, D. J. B. Lloyd, J. Burke, E. Knobloch, and B. Sandstede, *SIAM J. Appl. Dyn. Syst.* **9**, 704 (2010).
- [20] M. Pesch, E. Grosse Westhoff, T. Ackemann, and W. Lange, *Phys. Rev. Lett.* **95**, 143906 (2005).
- [21] M. Pesch, Ph.D. thesis, University of Muenster, 2006.
- [22] E. Meron, H. Yizhaq, and E. Gilad, *Chaos* **17**, 037109 (2007).
- [23] D. V. Skryabin and W. J. Firth, *Phys. Rev. E* **58**, R1252 (1998); D. E. Edmundson, *ibid.* **55**, 7636 (1997); J. M. Soto-Crespo, D. R. Heatley, E. M. Wright, and N. N. Akhmediev, *Phys. Rev. A* **44**, 636 (1991).
- [24] P. V. Paulau, D. Gomila, P. Colet, B. A. Malomed, and W. J. Firth, *Phys. Rev. E* **84**, 036213 (2011).
- [25] B. A. Malomed, D. Mihalache, F. Wise, and L. Torner, *J. Opt. B: Quantum Semiclass. Opt.* **7**, R53 (2005).
- [26] M. Sheintuch and O. Nekhamkina, *J. Chem. Phys.* **109**, 10612 (1998).
- [27] A. S. Mikhailov and K. Showalter, *Phys. Rep.* **425**, 79 (2006).
- [28] E. Mihaliuk, T. Sakurai, F. Chirila, and K. Showalter, *Phys. Rev. E* **65**, 065602(R) (2002).
- [29] G.-L. Oppo, *J. Math. Chem.* **45**, 95 (2009).
- [30] O. Bang, W. Krolikowski, J. Wyller, and J. J. Rasmussen, *Phys. Rev. E* **66**, 046619 (2002).
- [31] V. S. Zykov, H. Brandtstadter, G. Bordiougov, and H. Engel, *Phys. Rev. E* **72**, 065201(R) (2005).
- [32] H. Sakaguchi, *Phys. Rev. E* **64**, 047101 (2001).
- [33] L. Gelens, D. Gomila, G. Van der Sande, M. A. Matias, and P. Colet, *Phys. Rev. Lett.* **104**, 154101 (2010).
- [34] K. Pyragas, *Phys. Lett. A* **170**, 421 (1992).
- [35] M. Tlidi, A. G. Vladimirov, D. Pieroux, and D. Turaev, *Phys. Rev. Lett.* **103**, 103904 (2009).
- [36] P. V. Paulau, D. Gomila, P. Colet, M. A. Matías, N. A. Loiko, and W. J. Firth, *Phys. Rev. A* **80**, 023808 (2009).
- [37] F. Troeltzsch, *Optimal Control of Partial Differential Equations. Theory, Methods and Applications*, Vol. 112 (American Math. Society, Providence, 2010).
- [38] Y. S. Kivshar and B. A. Malomed, *Rev. Mod. Phys.* **61**, 763 (1989).
- [39] G. Flores, *J. Diff. Equat.* **80**, 306 (1989).
- [40] M. Argentina, P. Coulet, and V. Krinsky, *J. Theor. Biol.* **205**, 47 (2000).
- [41] I. Idris and V. N. Biktashev, *Phys. Rev. E* **76**, 021906 (2007).
- [42] R. Y. Chiao, E. Garmire, and C. H. Townes, *Phys. Rev. Lett.* **13**, 479 (1964).
- [43] Y. Nishiura, T. Teramoto, and K.-I. Ueda, *Chaos* **15**, 047509 (2005).